

Self-consistent pseudopotential calculations for sodium adsorption on GaAs(110)

Jörk Hebenstreit* and Matthias Scheffler

Fritz-Haber-Institut der Max-Planck-Gesellschaft, Faradayweg 4-6, D-1000 Berlin 33, Germany

(Received 10 April 1992)

We report self-consistent electronic structure, total-energy, and force calculations based on the density-functional theory for the Na adsorption on GaAs(110). In particular we studied three different coverages: $\Theta = \frac{1}{4}$, $\frac{1}{2}$, and 1 ($\Theta = 1$ means one adatom per substrate surface atom). We find that the Na core electrons play an important role for the exchange-correlation interaction and we therefore carry the atomic core-electron density of sodium along with the self-consistent calculations. Tests with our formulation of this core-valence exchange-correlation interaction are presented for the free sodium atom, the NaCl crystal, and Na metal. By the sodium adsorption on GaAs(110) the atomic and electronic structure of the substrate is locally changed, depending on the coverage. For $\Theta = \frac{1}{4}$ and $\frac{1}{2}$ the calculations give that the highest occupied Kohn-Sham band is rather flat and only partially occupied. We show that the Hubbard correlation energy of this band is larger than the bandwidth. We therefore conclude that the system should be described in a Hubbard picture rather than in a Bloch picture. As a consequence, it should be nonmetallic. The calculated values of the Schottky-barrier height and of the variation of phototreshold as a function of coverage are in good agreement with experimental data. From a detailed analysis of the surface electronic structure we explain the different Schottky-barrier behavior for *p*-type and *n*-type substrates.

I. INTRODUCTION

Metal-semiconductor interfaces have been studied for decades,^{1,2} in order to explore the mechanism and properties of the formation of Schottky barriers. Of particular interest is the interdependence of the interface atomic geometry and electronic structure. Despite enormous research activities several fundamental aspects of Schottky barriers are still poorly understood and a matter of active controversies. Among the basic questions which are still under debate are those about the mechanism of the Fermi-level pinning at very low coverages, the mechanism of the shift of the Fermi level as a function of coverage, and the character of the states responsible for the Fermi-level pinning. Several concepts have been suggested to explain the Fermi-level pinning. These concepts can be classified into two main groups. First, there is the concept of *metal-induced gap states* (MIGS) proposed by Heine³ that explains the Fermi-level pinning by intrinsic surface states of the semiconductor substrate which are perturbed due to the presence of the metal adatoms at the surface. Based on the MIGS idea, Tejedor, Flores, and Louis⁴ developed the *induced density of interface state* model (IDIS). The *neutrality level* and *average hybrid energy* of Harrison and Tersoff⁵ also describe the same physical mechanism as the MIGS. Second, there is the *unified defect model* (UDM) proposed by Spicer *et al.*^{6,7} that explains the Fermi-level pinning due to gap states related to structural semiconductor defects. Recently Mönch⁸ discussed a model combining defect-related states and MIGS to describe the Fermi-level pinning at different coverages.

The aim of the present study is to apply accurate self-consistent total-energy calculations to determine the

character of the states which pin the Fermi level in the range of submonolayer coverages. In order to predict the Fermi-level pinning and thus the Schottky-barrier height from a theoretical point of view, it is necessary to know the electronic structure of the metal-covered semiconductor surface. As the electronic structure is closely related to the atomic geometry it is crucial to determine the atomic positions of the semiconductor substrate and of the adsorbate atoms. Our theoretical approach therefore optimizes both the atomic and the electronic degrees of freedom of the Na adsorbate on GaAs(110).

Among the metal-semiconductor interfaces studied in the past decades, those based on III-V compounds as substrate are most intensively investigated. In our work we explore a sodium-covered GaAs(110) surface. There are several reasons to consider an alkali-covered GaAs(110) surface. First, GaAs(110) is one of the best understood semiconductor surfaces, both experimentally and theoretically (for a discussion see Ref. 9 and references therein). Second, there is a particular interest in understanding the alkali adsorption because they reduce the work function significantly. Nevertheless, the Schottky-barrier heights of alkali-semiconductor junctions are roughly the same as those of other metal-semiconductor junctions. Third, the rather simple electronic configuration of alkali atoms makes them attractive candidates for a theoretical description of metal-semiconductor interfaces.

Through this paper we define the coverage such that $\Theta = 1$ corresponds to a GaAs(110) adatom density of 8.85×10^{14} atom/cm², i.e., it corresponds to two adsorbate atoms per pair of Ga and As atoms on the surface. *One monolayer*, on the other hand, means a close-packed layer of adatoms and, therefore, depends on the size of the particular adatom. In the case of sodium, one mono-

layer (ML) corresponds to $\Theta = 1$.

Alkali adsorption on GaAs(110) surfaces has been studied intensively in recent years. Among the alkali adsorbates Cs was investigated most. Scanning tunneling microscopy (STM) experiments of a Cs-covered GaAs(110) surface identified one-dimensional adsorbate-induced chains, even for coverages Θ as low as 0.03.^{10,11} A particular clear picture of the chains is obtained for experiments with a negative sample bias which implies that electrons are measured which tunnel out from occupied states of the sample. The chains are observed to be several hundred angstroms long. The authors attribute the maxima of the topographic images to the Cs adatoms which are approximately centered within four surface As atoms. The existence of one-dimensional structures indicates an anisotropic interaction between the adatoms which is *attractive* along the atomic chains of the substrate, i.e., the $[1\bar{1}0]$ direction.¹⁰ At increased coverages different overlayer structures are found, starting with the one-dimensional chains, then forming two-dimensional structures, and finally three-dimensional Cs growth.¹¹ The existence of different geometric arrangements on the surface seems to be confirmed by Auger-electron spectroscopy.¹² Still, a detailed understanding of the atomic arrangements at the surface is lacking. This is particularly so because the alkali substrate interaction is often described in terms of a partial charge transfer of the outermost *s* electron from the adatom to the substrate resulting in a system of *repulsive* monopoles and dipoles at low coverages. Therefore, one expects at low coverages *disordered* overlayer structures, i.e., no island or chain formation.

Whitman *et al.*¹¹ also searched at the Cs-covered GaAs(110) surface for metallic characteristics. Current-versus-voltage measurements over the one-dimensional chains and two-dimensional overlayer structures reveal that these structures are insulating. Interfaces which are formed by growing a second Cs layer clearly exhibit metallic behavior, i.e., a finite conductivity at zero bias in STM which originates from partially occupied states at the Fermi level.^{11,12} Using electron-energy-loss spectroscopy (EELS), DiNardo *et al.*¹³ investigated the semiconductor-to-metal transition at the Cs-covered GaAs(110) surface. At low coverages ($\Theta < 0.25$) no electronic losses were found in the band gap. At coverages $\Theta \geq 0.25$, two loss features appear in the GaAs band gap, which energies do not change up to saturation coverage (i.e., $\Theta = 0.45$). The authors attribute these losses to localized states, but they dismiss isolated defects as the origin of these features. With further increase of coverage a new loss appears which shifts in energy, and an excitation continuum fills the band gap. This indicates that for coverages $\Theta \geq 0.5$ the surface becomes metallic,¹³ i.e., the metallization starts when the second overlayer growth. The nonmetallic behavior of alkali-covered GaAs(110) surfaces for submonolayer coverages is also confirmed by photoemission experiments.^{14–17} With this technique, no density of states is found at the Fermi level. In contrast to these experimental findings, recent theoretical results show a significant density of states at the Fermi level^{18,19} and the authors therefore concluded that the interface is

metallic even at submonolayer coverages.¹⁸

We present results of parameter-free, self-consistent pseudopotential calculations based on the density-functional theory,^{20,21} applying the local-density approximation.^{22,23} It is noted that a proper treatment of the exchange-correlation potential is very important. A linearization of the core-valence exchange-correlation functional, as it is usually applied in pseudopotential calculations, is not an appropriate approximation for alkalis²⁴ and induces significant errors in the calculated atomic and electronic structure. It is therefore necessary to take a part of the alkali core electrons into account along with the self-consistently calculated valence-electron density to calculate the exchange-correlation energy and potential.

The paper is organized as follows. After Sec. II, which describes our theoretical approach, we discuss in Sec. III the sodium pseudopotential along with its applications to the Na atom, the NaCl crystal, and Na metal. In Sec. IV we present the results for the sodium-covered GaAs(110) surface for different coverages: $\Theta = \frac{1}{4}$, $\frac{1}{2}$, and 1. A discussion concerning the metallization of the surfaces, the variation of the Schottky barrier, and the photothreshold as a function of coverage, as well as the different Schottky-barrier behavior for *n*-type and *p*-type substrates, are presented in Sec. V. Finally, the paper is concluded with a summary in Sec. VI.

II. OUTLINE OF THE THEORETICAL METHOD

We perform parameter-free electronic structure, total-energy, and force calculations based on the density-functional theory (DFT) (Refs. 20 and 21) and using the local-density approximation (LDA) for the exchange-correlation functional.^{22,23} The electron-ion interaction is described by norm-conserving, fully separable pseudopotentials.^{25,26} As a modification to the potentials given in Ref. 26 we changed the sodium *ionic* pseudopotential by taking into account part of the core electrons for the exchange-correlation potential (see Sec. III). A plane-wave basis set is used to represent the single-particle orbitals of the valence electrons.

We use the repeated-slab method²⁷ to simulate the semiconductor surface. The system is periodic parallel to the surface and we introduce an artificial periodicity perpendicular to the surface, defining a large three-dimensional unit cell. The number of layers in the unit cell and its size parallel to the surface depends on the coverage which is studied. For the coverages $\Theta = \frac{1}{2}$ and 1 our slab contains eight layers of GaAs(110) 1×1 and a vacuum region equivalent in thickness to six such layers. In the case of $\Theta = \frac{1}{4}$ each slab contains seven layers of GaAs(110) 1×2 and a vacuum equivalent to seven layers. Figure 1 shows the top view on both slabs. Sodium atoms were placed on both sides of the slab. For the plane-wave basis set we use an energy cutoff equal to 8 Ry which corresponds to about 1500 plane waves for the small slab and about 3000 plane waves for the large slab. The *k*-space integration is replaced by a sum of four special *k* points²⁸ of the irreducible part of the surface Brillouin zone. To improve the *k*-space sampling we use par-

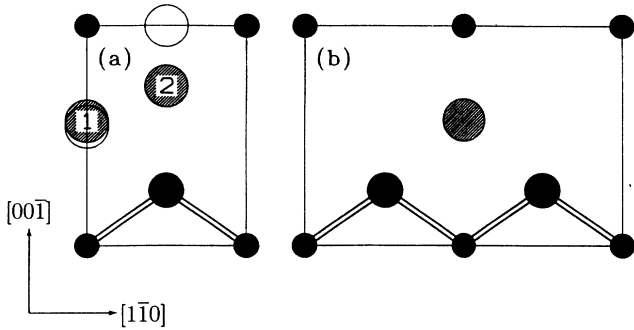


FIG. 1. Top view on the surface unit cell of (a) a small slab and (b) a large slab together with possible sodium adsorption sites. Large circles indicate As atoms and small circles indicate Ga atoms. Hatched circles mark stable adsorption positions for the $\Theta = \frac{1}{2}$ coverage [in (a)] and for the $\Theta = \frac{1}{4}$ coverage [in (b)]. Large open circle indicate the equilibrium adatom positions for the $\Theta = 1$ coverage.

tial occupation numbers according to a Fermi function with a width of $kT^{\text{el}} = 0.01$ eV. The results in a previous paper were obtained with $kT^{\text{el}} = 0.1$ eV. Due to this change and due to some numeric inaccuracies in our earlier force calculation the present results differ in some details from those of Ref. 29.

The GaAs lattice constant is optimized for a GaAs(110) 1×1 slab using the above-mentioned parameters. All results reported hereafter were obtained with this theoretical lattice constant of 5.5 Å (the experimental value is 5.65 Å). Zero-point motion is not considered in the theoretical value. In order to determine the equilibrium atomic positions for the surface calculation the three outermost layers of atoms on both sides of the slab were relaxed to geometries given by the calculated total energy and forces, using an “optimized steepest descent” method for the atomic displacements together with a Car-Parrinello³⁰-like approach for bringing the wave functions to self-consistency. The equilibrium geometry is identified when all forces are smaller than 0.005 eV/Å. This corresponds to a numerical uncertainty of the atomic positions of less than 0.05 Å.

III. SODIUM PSEUDOPOTENTIAL AND ITS APPLICATION IN BULK CALCULATIONS

The pseudopotential concept starts from the assumption that only valence electrons contribute to the chemical bonding. Therefore, only the valence-electron density is varied in the self-consistent solution of the Kohn-Sham equation, while the core electrons are hidden in the pseudopotential. This is particularly simple if one can linearize the core-valence exchange-correlation functional:

$$E_{\text{xc}}[\rho^{\text{core}} + \rho^{\text{val}}] \approx E_{\text{xc}}[\rho^{\text{core}}] + E_{\text{xc}}[\rho^{\text{val}}]. \quad (1)$$

However, this approximation is not acceptable for treating alkalis,²⁴ because the valence s and p orbitals overlap with the core orbitals. Following the approach of Louie, Froyen, and Cohen,²⁴ we therefore create an ionic pseudopotential (with the parameters of Ref. 26) subtracting not only the exchange-correlation potential of the valence

electrons from the atomic pseudopotential, but also taking part of the core electrons into account. In order to describe the nonlinear core-valence exchange-correlation interaction, only that part of the core-charge density which has a significant overlap with the valence-charge density is important. On the other hand, the core charge is strongly localized, which would lead to very hard pseudopotentials that in turn require large plane-wave basis sets. Therefore, the core-charge density is smoothed within a radius of $r \leq r_c = 1.3$ Å by fitting a parabola to the total core-charge density at $r = r_c$ and leaving it unchanged outside this radius. Table I lists the smoothed core-electron density, $\bar{\rho}^{\text{core}}$, as a function of the distance. The new ionic pseudopotential, depending on the angular momentum quantum number l , is then written as

$$V_l^{\text{ps-ion}} = V_l^{\text{ps-atom}} - V_{\text{H}}(\rho^{\text{ps-val}}) - V_{\text{xc}}(\bar{\rho}^{\text{core}} + \rho^{\text{ps-val}}). \quad (2)$$

Note that for the calculation of the p and d atomic pseudopotential, ionic configurations are considered,³¹ otherwise the p and d electrons would not be bound by the pseudopotential. Therefore the pseudo-valence-charge $\rho^{\text{ps-val}}$ is also l dependent. This is, however, a detail and therefore it is not noted in Eq. (2). We note that the atomic pseudopotential for sodium remains unchanged by this approach and therefore the logarithmic derivatives of the atomic pseudo-wave-functions remain the same as given in Ref. 26.

Our calculated ionic pseudopotential is tested for the free-sodium atom, the NaCl crystal, and the Na bulk. For the free atom we compare the behavior of the $3s$ eigenvalue as a function of the occupation of the $3s$ orbital (Fig. 2) obtained with an all-electron calculation (dotted line) and self-consistent pseudopotential calculations with (solid line) and without (dashed line) the nonlinear correction for the exchange-correlation energy, solving the radial Schrödinger equation. In all three calculations we ob-

TABLE I. Smoothed core-electron density $\bar{\rho}^{\text{core}}(r)$ as a function of distance.

| r (bohr) | $\bar{\rho}^{\text{core}}(r)$ (bohr ⁻³) | r (bohr) | $\bar{\rho}^{\text{core}}(r)$ (bohr ⁻³) |
|------------|---|------------|---|
| 0.000 909 | 0.255 868 | 2.344 685 | 0.026 870 |
| 0.103 269 | 0.255 406 | 2.461 919 | 0.017 556 |
| 0.204 465 | 0.254 058 | 2.585 015 | 0.011 283 |
| 0.302 088 | 0.251 917 | 2.714 266 | 0.007 128 |
| 0.404 827 | 0.248 773 | 2.849 979 | 0.004 423 |
| 0.516 673 | 0.244 311 | 2.992 478 | 0.002 693 |
| 0.628 020 | 0.238 793 | 3.142 102 | 0.001 608 |
| 0.727 011 | 0.232 985 | 3.299 207 | 9.397×10^{-4} |
| 0.927 871 | 0.218 595 | 3.464 167 | 5.374×10^{-4} |
| 1.022 978 | 0.210 562 | 3.637 376 | 3.002×10^{-4} |
| 1.127 833 | 0.200 799 | 3.819 244 | 1.637×10^{-4} |
| 1.243 436 | 0.188 931 | 4.010 207 | 8.694×10^{-5} |
| 1.370 889 | 0.174 506 | 4.210 717 | 4.493×10^{-5} |
| 1.511 405 | 0.156 972 | 4.421 253 | 2.256×10^{-5} |
| 1.666 324 | 0.135 659 | 4.642 315 | 1.099×10^{-5} |
| 1.837 122 | 0.109 754 | 4.874 431 | 5.184×10^{-6} |
| 1.928 978 | 0.094 777 | 5.118 153 | 2.364×10^{-6} |
| 2.025 427 | 0.078 265 | 5.374 060 | 1.040×10^{-6} |
| 2.126 698 | 0.060 061 | 5.642 763 | 4.407×10^{-7} |
| 2.233 033 | 0.040 480 | 5.924 902 | 1.795×10^{-7} |

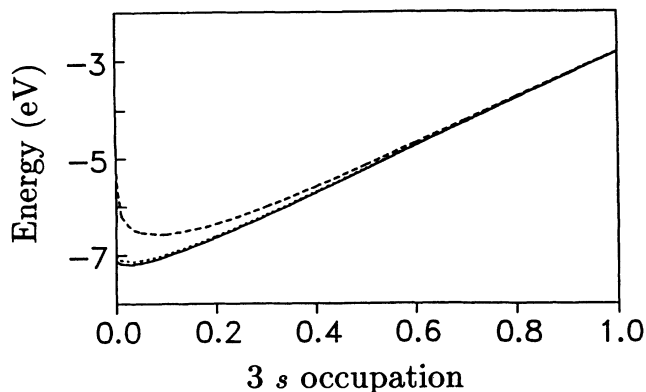


FIG. 2. Energy of the 3s orbital of the free Na atom as a function of its occupation obtained from an all-electron calculation (dotted line) and pseudopotential calculations with (solid line) and without (dashed line) the nonlinear correction for the exchange-correlation energy.

tain almost the same eigenvalue when the 3s orbital is occupied with more than 0.7 electrons. Note that there is a deviation of as much as 1.8 eV between the core-valence linearized pseudopotential and the all-electron calculation when the 3s orbital is empty. This implies that, when the Na atom becomes ionized, the 3s orbital energy is significantly incorrect. With the standard procedure of pseudopotential theory [see Eq. (1)] we obtained a lattice constant for the NaCl crystal which is too small by 35% compared to experiment. Including the core correction, the correct behavior of the 3s eigenvalue of the free Na atom as a function of the occupation is well reproduced (compare Fig. 2) and the lattice constant for NaCl is found to be 5.67 Å [the experimental value is 5.64 Å (Ref. 32)]. No correction for zero-point motion is considered in the calculations. Froyen and Cohen³³ obtained a slightly smaller lattice constant (5.52 Å) with a similar method. It is obvious that the large mistake in the lattice constant of a calculation which linearizes the core-valence exchange-correlation interaction influences the band structure of the NaCl crystal. In Fig. 3 we show the band structure with (lower panel) and without (upper panel) the correction. The calculated band structure without the core correction shows that the NaCl would behave like a semimetal instead of being an insulator. Beside the dramatic reduction of the gap, the sequence of the energy levels in the conduction band is reversed. If the core-valence exchange correlation is treated properly, the dispersion of calculated bands agrees well with previous calculations performed with an empirical pseudopotential³⁴ and with the self-consistent calculations of Froyen and Cohen.³⁵ However, compared to the empirical and experimental data, our energy gap is too small, but this is the known DFT-LDA effect.

The above-mentioned results for NaCl are obtained by self-consistent bulk calculations using an energy cutoff of 40 Ry, a set of 10 special \mathbf{k} points²⁸ in the irreducible part of the Brillouin zone, and the Ceperley-Alder results for the exchange-correlation functional.^{22,23} We also performed calculations for a bcc Na crystal. For these calculations we use a set of 40 special \mathbf{k} points,²⁸ an energy

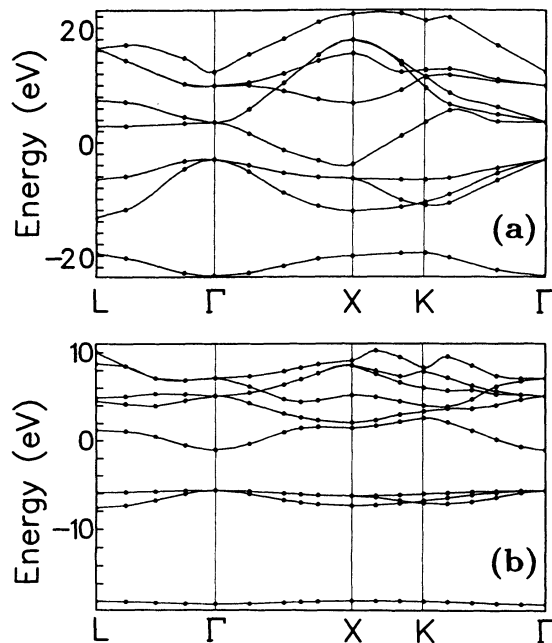


FIG. 3. Band structure for NaCl (a) without and (b) with the nonlinear correction for the exchange-correlation energy.

cutoff of 12 Ry, and the same exchange and correlation functional as above. The Na lattice constant is found to be 4.02 Å, which is slightly smaller than the value obtained with an all-electron calculation (4.08 Å) (Ref. 36) and about 4.5% smaller than the experimental value (4.20 Å).³² The calculated bulk modulus is $B_0 = 0.105$ Mbar. In Table II the main results for NaCl and Na metal are compiled and compared to other theoretical and to experimental data.

TABLE II. Lattice constant and bulk modulus for NaCl and Na metal compared to other theoretical results and experimental data. In the theoretical lattice constant the zero-point motion is not taken into account. B_0 is calculated at a_0 .

| | Lattice constant a_0 (Å) | Bulk modulus B_0 (Mbar) |
|---|-------------------------------|------------------------------|
| NaCl | | |
| Present paper | 5.67 | 0.286 |
| Froyen and Cohen (Ref. 33) | 5.52 | 0.312 |
| Experiment | 5.64 ^a | 0.266 ^b |
| Na | | |
| Present paper | 4.02 | 0.105 |
| Louie, Froyen, and Cohen (Ref. 24) | 4.09 | 0.095 |
| Moruzzi, Janak, and Williams (Ref. 36) | 4.08 | 0.090 |
| Experiment | 4.20 ^c | 0.068 ^d |

^aReference 32.

^bReference 37.

^cReference 38.

^dReference 39.

IV. SODIUM COVERED GaAs(110)

A. The atomic geometry for different coverages

For a detailed understanding of the surface or interface electronic properties it is necessary to know the atomic geometry. There is an ongoing debate of how alkali adatoms remove or modify the substrate relaxation. In previous calculations the substrate was assumed to be completely unrelaxed, thus having the geometry of a truncated bulk,^{18,19} but a proof for this assumption is missing. In fact, we have shown that this assumption is incorrect.²⁹ We now discuss our results for Na/GaAs(110) for three different coverages, i.e., $\Theta = \frac{1}{4}$, $\frac{1}{2}$, and 1. We start with the clean relaxed surface, adsorb the sodium layer on each side of the slab, and then relax the atomic and electronic degrees of freedom.

1. The coverage $\Theta = \frac{1}{2}$

In order to determine the equilibrium adsorbate positions and the substrate surface geometry we evaluate the Born-Oppenheimer total-energy surface for the $\Theta = \frac{1}{2}$ coverage. For about 30 adatom positions (adsorbate coordinates fixed parallel to the surface) within the two-dimensional surface unit cell [Fig. 1(a)] the adsorbate-surface distance as well as the atomic positions of the top three substrate layers are fully relaxed. For a clearer graphical presentation we show in Fig. 4 the total-energy surface over an area of two surface unit cells. The Born-Oppenheimer surface exhibits deep channels which go parallel to the surface atomic chains, i.e., along the $[1\bar{1}0]$ direction.²⁹ Along such a channel we find two minima within the surface unit cell [labeled as “site 1” and “site 2” in Figs. 1(a) and 4(b)] separated by a small barrier of about 0.2 eV. Perpendicular to the channel the energy barrier is calculated as 0.7 eV. One minimum in the total energy is found to be in the Ga rows (along the $[00\bar{1}]$ direction) of the surface almost halfway between consecutive Ga atoms (site 1). The other minimum lies in the As rows of the surface (site 2). We obtain adsorption energies of 1.77 eV for both minima. The adsorption energy is calculated as the difference between the total energies of the sodium-covered surface, the clean *relaxed* surface, and the free Na atom. It is taken as positive when adsorption is favorable. The total energy of the free atom is obtained with the same energy cutoff and the same exchange-correlation functional as for the adsorbate system. Taking spin-polarization effects of the sodium atom into account, the adsorption energy would be reduced by 0.2 eV.

Upon adsorption the relaxation of the clean surface is reduced although a significant buckling of about 0.2 Å remains (see Table III): The Ga atoms are pushed back almost to their bulk positions whereas the As atoms remain practically unchanged at their positions of the relaxed surface.

2. The coverage $\Theta = \frac{1}{4}$

The $\Theta = \frac{1}{4}$ coverage is treated with a GaAs(110) 1×2 slab [see Fig. 1(b)]. The total-energy surface for this cov-

erage was calculated for several positions within the surface unit cell, which shows that the topology is practically the same as in the previous studied case (Fig. 4). Again we find a minimum in the Ga rows of the surface corresponding to an adsorption energy of 1.8 eV. Contrary to the results of the previous paragraph, we find, however, that a minimum at site 2 is not developed: The bottom of the valley in the total-energy surface now has a quite broad plateau, with a saddle point in the As rows separating two consecutive minima in the Ga rows. The difference between the adsorption energies at the saddle point and at the minimum is just the energy barrier, i.e., 0.2 eV. The barrier perpendicular to the channels is again 0.7 eV, as in the $\Theta = \frac{1}{2}$ case.

The analysis of the atomic geometry shows that the substrate relaxation is changed mainly for the nearest neighbors of the adatom (see Table III). The Ga atom close to the adsorbate is back close to its bulk position, whereas the Ga atom further away from the adsorbate

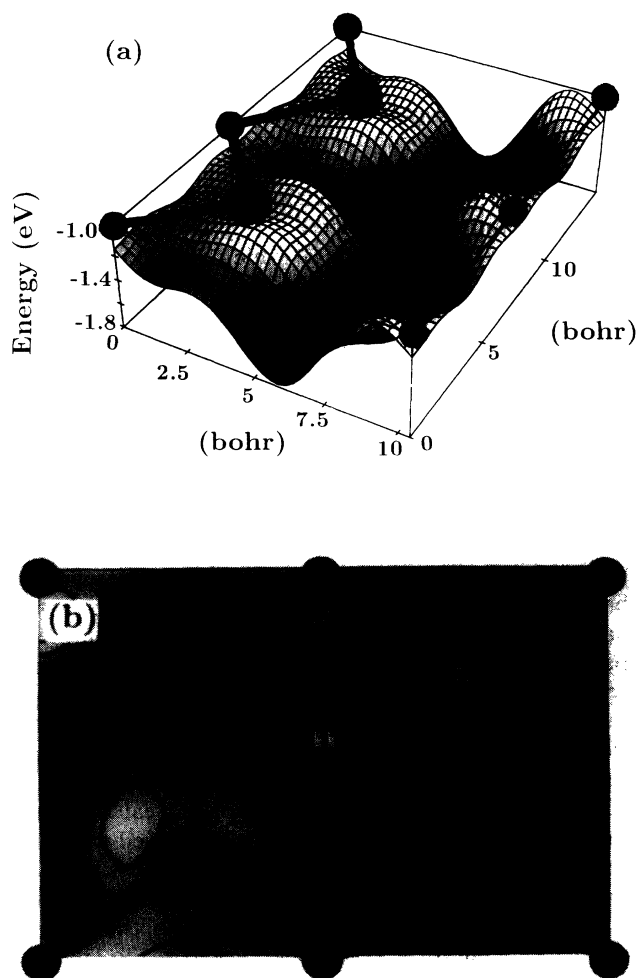


FIG. 4. Total-energy surface of the $\Theta = \frac{1}{2}$ Na/GaAs(110) system. (a) Three-dimensional perspective view and (b) contour plot together with the projected surface atomic positions. Large circles indicate As atoms and small circles mark the Ga atoms. In the contour plot the channel in the total-energy surface is drawn dark grey. The labels “1” and “2” indicate stable adsorption positions for the $\Theta = \frac{1}{2}$ coverage.

TABLE III. Atomic displacements along the ($[1\bar{1}0]$, $[00\bar{1}]$, $[110]$) directions with respect to the truncated bulk geometry in angstroms. The Na positions are given with respect to a surface Ga site of the unrelaxed geometry. In the $\Theta = \frac{1}{4}$ case the \pm sign indicates that both As neighbors move towards the Na adsorbate, the data in the first line refer to the atoms further away from the adatom, and the data in the second line refer to the atoms next to the adatom.

| | Na | Ga | First layer As |
|---------------------------------|------------------|--------------------|--------------------------|
| Clean surface | | (0.30,0.00, -0.40) | (0.07,0.00,0.23) |
| $\Theta = \frac{1}{4}$ | (3.14,0.00,1.48) | (0.37,0.00, -0.39) | |
| | | (0.11,0.00, -0.11) | (0.08, \pm 0.02, 0.20) |
| $\Theta = \frac{1}{2}$ (site 1) | (3.10,0.00,1.36) | (0.10,0.00,0.00) | (0.07,0.00,0.17) |
| $\Theta = \frac{1}{2}$ (site 2) | (4.00,1.95,1.35) | (0.19,0.00, -0.05) | (0.11,0.00,0.22) |
| $\Theta = 1$ | (2.96,0.00,1.38) | (0.05,0.00,0.14) | (0.09,0.00,0.11) |
| | (5.39,1.95,2.47) | | |

remains at its position of the clean relaxed surface. The surface As atoms are slightly pulled towards the adsorbate along the $[1\bar{1}0]$ direction, which, for the other coverages studied in this work, is forbidden by symmetry. Their distance from the ideal surface as well as their displacement in the $[00\bar{1}]$ direction are essentially the same, as in the case of the clean relaxed surface. Therefore, the buckling of the surface is practically the same as for the clean relaxed surface.

3. The coverage $\Theta = 1$

For this coverage we take again the GaAs(110) 1×1 slab, placing two sodium atoms per pair of Ga and As atoms on the surface. We start from a configuration where one atom is located at site 1 and the other at site 2 of the $\Theta = \frac{1}{2}$ case. It turned out that the adatom position at site 1 is changed only a little, whereas the atom at site 2 is shifted to a position where it bridges two Ga atoms in the $[1\bar{1}0]$ direction. Therefore this adatom sits much higher than the other one (see Table III). The adsorption positions for the $\Theta = 1$ coverage are indicated by large open circles in Fig. 1(a). Both the Ga and the As atoms of the substrate are now essentially planar but the interlayer distance between the first and second substrate layer is increased by about 6% compared to the bulk interlayer distance. In this configuration the smallest adatom-adatom distance is about 5% shorter than the distance in bulk bcc sodium; see Sec. III above. We like to mention that these results correspond to a minimum of the total energy. However, we cannot rule out that for this ($\Theta = 1$) coverage other minima exist as well. This may be of interest of future investigations.

If we compare the results of Secs. IV A 1–IV A 3 we conclude that a single sodium atom can move rather freely on the GaAs(110) substrate with low migration barriers, but the diffusion should be highly anisotropic, i.e., the adatom will move mainly in the $[1\bar{1}0]$ direction of the surface. This result may explain the existence of one-dimensional adatom structures in the low coverage regime as they are visualized with STM.^{10,11} On the other hand, a comparison of the adsorption energies per adatom (Table IV) shows that for all coverages the energy gain is of the same order, although the $\Theta = \frac{1}{2}$ coverage is

slightly less favorable. This indicates that the adatom-adatom interaction is not strongly repulsive and contradicts the common picture of alkali adsorption on semiconductors.

For low coverages we expect an adsorption in a more open structure with a local coverage of $\Theta = \frac{1}{4}$. The most favorable adsorption site is that close to the surface Ga atoms, marked by a hatched circle in Fig. 1(b). For higher adatom concentrations, i.e., $\Theta > \frac{1}{4}$, a local coverage equivalent to one monolayer seems to be favorable. The distance between the adsorbate and the surface Ga atom is almost the same for all adatom geometries studied in this paper (Table IV), i.e., about 2.9 Å.

B. Electronic properties

The calculated surface band structures are shown in Fig. 5 for the three coverages studied in this work. The hatched region indicates the projected bulk band structure and solid lines represent surface features. The occupation of the highest occupied and the lowest unoccupied state is indicated with full and open circles, respectively.

1. The coverage $\Theta = \frac{1}{4}$

In the surface band structure of our $\Theta = \frac{1}{4}$ system we identify three surface states in the region of the fundamental band gap. The lowest one is a fully occupied As-derived state close to the valence-band top. The two other states are Ga related surface states. The lower one is occupied with one electron and therefore it determines the Fermi level. The corresponding wave function is lo-

TABLE IV. Comparison of the adsorption energies per adatom E_{ad} and the distances d_{Na-Ga} between the adatom and the surface-Ga atom for different coverages.

| | E_{ad} (eV) | d_{Na-Ga} (Å) |
|---------------------------------|------------------|--------------------|
| $\Theta = \frac{1}{4}$ | 1.88 | 2.93 |
| $\Theta = \frac{1}{2}$ site (1) | 1.77 | 2.84 |
| $\Theta = \frac{1}{2}$ site (2) | 1.77 | 2.93 |
| $\Theta = 1$ | 1.87 | 2.87,3.04 |

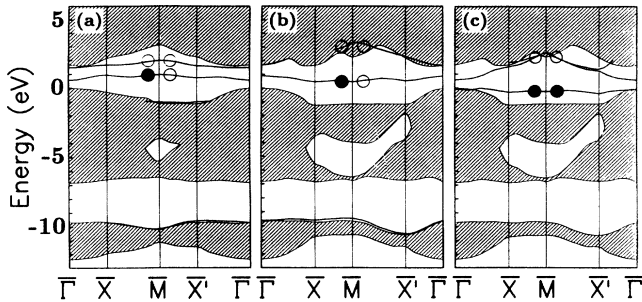


FIG. 5. Calculated surface band structures for the Na/GaAs(110) system for the coverages studied in this paper: (a) $\Theta = \frac{1}{4}$, (b) $\Theta = \frac{1}{2}$, and (c) $\Theta = 1$. The hatched region shows the projected bulk band structure and the solid lines indicate surface features. The occupation of the highest occupied and the lowest unoccupied state are indicated by full and open circles. Note that the band structure for $\Theta = \frac{1}{4}$ is plotted on a different scale, because the surface Brillouin zone is half as large as in the other cases.

calized mainly at the Ga atom, which is close to the adsorbate. The upper state is an empty state which is localized at the Ga surface atom further away from the adatom. For a more detailed discussion of the character of these Ga states see Sec. IV B 2, which deals with a different coverage but which is still sufficiently low such that the wave functions of the Ga derived state is essentially unchanged.

From the difference of the electron density of the sodium-covered surface and the clean surface we can analyze how the electronic structure at the surface is changed by the sodium adsorption. For this comparison the electron density of the clean surface is calculated with the same atomic geometry as for the $\Theta = \frac{1}{4}$ Na/GaAs(110) system. Figure 6 shows the difference plotted in a plane parallel to the surface at a distance halfway between the ideal surface and the adatom position. The positions of the surface atoms and of the adatom are projected on this plane. The figure demonstrates that the sodium adatom influences mainly the electron density of its first neighbors. There is a large increase in the charge density between the surface Ga atom and the adatom. This is understood such that the Na 3s electron is transferred into an orbital which has significant weight between the Ga atom and the Na adatom. We also find an increase of charge density between the adsorbate and the surface As atoms as a result of a polarization of the rather high As electron density.

2. The coverage $\Theta = \frac{1}{2}$

In Fig. 5(b) there are two surface states in the fundamental band gap. The single occupied state is a Ga derived state²⁹ and determines the Fermi level. The wave function of this state is shown in the left panel of Fig. 7. From this plot it is obvious that the character of the half-occupied state of Fig. 5(b) is very similar to that of a

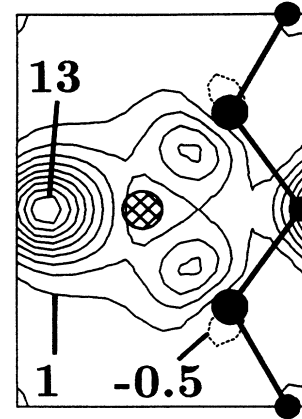


FIG. 6. Change of surface electron density due to $\Theta = \frac{1}{4}$ Na adsorption. This is the difference in electron density of the sodium-covered system and a clean surface, using the same surface atomic geometry for both calculations. The plot shows a cut along a (110) plane at a distance halfway between the ideal surface and the adatom. The positions of the surface atoms as well as of the adatom are projected on this plane and are indicated by a large hatched circle (Na), large full circles (As), and small full circles (Ga). Negative values of the charge-density difference are indicated by dashed lines. Units are 10^{-3} bohr⁻³.

Ga dangling-bond state of the clean surface (see Ref. 9). Thus, the Na-GaAs(110) interaction is well characterized as follows: The Na 3s electron is donated from the sodium into a Ga dangling bond. This results in a partial ionization of the adatom. Nevertheless, because of the orbital character of the Ga dangling bond, the bonding between the Na and the surface Ga atom has a significant covalent character. Figure 5(b) shows that this Na-Ga derived state has a very small dispersion, which indicates that the orbitals localized at consecutive Ga atoms do not overlap significantly, in agreement with the left panel of Fig. 7.

The lowest unoccupied state has a completely different character (right part of Fig. 7). It is mainly localized on the vacuum side of the sodium atoms and has some small contributions at the substrate atoms of both species. This state could be understood as a mixture of Na 3s and 3p orbitals with some weak antibonding contribution from the Ga dangling orbital. The top right panel shows a cut along a plane parallel to the surface outside the Na position (indicated by the dotted line in the lower panel). Note that this band has an essentially one-dimensional extension with almost no variation of the charge density along the $[1\bar{1}0]$ direction.

3. The coverage $\Theta = 1$

At the $\Theta = 1$ coverage we find three states in the fundamental band gap. The lower one is occupied with two electrons. The upper two states are empty. Therefore the Fermi energy lies just in the middle of the resulting

surface band gap. We find that the character of the occupied state is very similar to that of the partially occupied state found for the other coverages, although the orbitals of the surface As atom are now somewhat more involved than before. Thus, this state is still a bonding state mainly built from the Ga dangling orbital. The character of the upper two states is more difficult to understand. They can be characterized as nonbonding combinations of dangling orbitals of the surface atoms and the adsorbate orbitals. In contrast to the band structures of the submonolayer coverages, now the unoccupied states are shifted from the bottom of conduction band to the center of the bulk GaAs band gap. Note that for the atomic geometry calculated in this study the surface is nonmetallic at this coverage.

From the analysis of the electronic structure we conclude that the system can be understood such that the sodium valence electron is transferred into the Ga-like surface state, which results in a partial ionization of the adatom. On the other hand, we find that the adsorption energies per adatom are about the same for all coverages studied in this paper. This clearly indicates that the

direct ion-ion repulsion is efficiently screened. This is possible because the transferred electron stays close to the Na nucleus (in the nearest Ga dangling orbital), and the changes in the surface atomic geometry (see Sec. IV A) together with the polarization of the As atoms screen the interaction. From the adsorption-induced electron-density change the screening length is estimated to be of the order of the nearest-neighbor distance both parallel to the surface as well as perpendicular to the surface.

V. SURFACE METALLIZATION, SCHOTTKY BARRIER, AND PHOTOTHRESHOLD

As discussed in the Introduction, the alkali-covered GaAs(110) surface is experimentally found to behave nonmetallic for coverages less than or equal to one monolayer.¹⁵ From the experiments one knows that the onset of metallization happens for coverages between one and two monolayers, i.e., the metallization occurs when the second adatom layer grows.^{11,13,15} Contrary to that, previous theoretical studies concluded that the surface is metallic even in the submonolayer case¹⁸ because of a significant density of states at the Fermi level. Our calculations show that the surface covered with one monolayer sodium ($\Theta=1$) is nonmetallic [see Fig. 5(c)]. There is a gap between occupied and unoccupied states of about 0.7 eV. If we compare this gap with the band gap of the clean surface, we can conclude that the full monolayer sodium coverage reduces the band gap by about 1 eV. This reduction in the gap size may be compared with experimental results of Whitman *et al.*¹¹ for the 1 ML of Cs (i.e., $\Theta=0.4$)-covered GaAs(110) surface. This comparison is meaningful because, due to the different sizes of Na and Cs, the adsorbate-adsorbate interaction of $\Theta_{\text{Na}}=1$ and $\Theta_{\text{Cs}}=0.4$ is comparable. The experimental result for Cs is 0.8 eV and thus consistent with our value of 1 eV for Na.

In the band structures of the submonolayer coverages [Figs. 5(a) and 5(b)] the calculations predict singly occupied states in the fundamental band gap which will pin the Fermi level. From this result one may conclude on a metallic behavior of the surface. However, we also see that this state has a very small dispersion over the surface Brillouin zone which indicates that the corresponding wave function is built from practically nonoverlapping orbitals. The wave-function analysis confirms this conclusion (see Fig. 7, left). Because of the localized character of the wave functions, the properties of this state should be discussed in a localized Hubbard picture, rather than in a delocalized Bloch picture.

It is interesting to note that DFT-LDA theory typically gives a good description of the ground-state electron density. However, the interpretation of Kohn-Sham orbitals or "bands" is less clear. In order to determine if the Bloch or Hubbard description is valid, we have to evaluate the Hubbard correlation energy of the state in Fig. 7 (left) and we have to compare this result with the calculated bandwidth W of this Kohn-Sham single-particle state. To estimate the correlation energy for the single occupied dangling-bond state in the fundamental

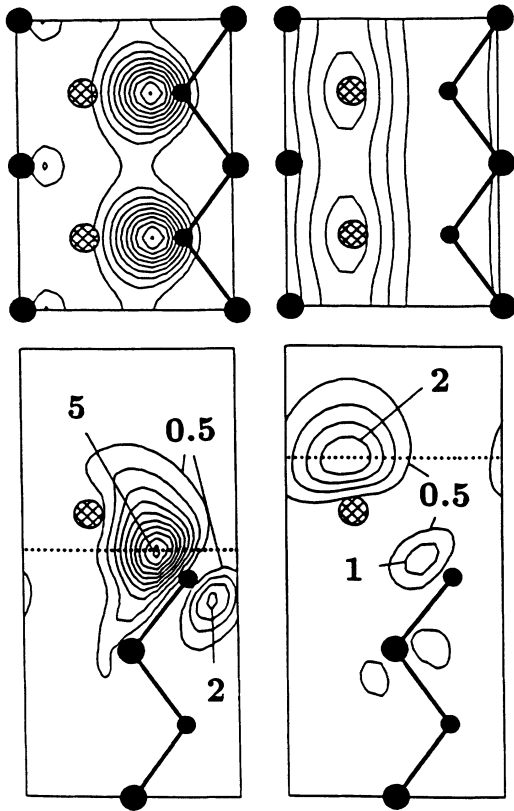


FIG. 7. Squared wave functions for $\Theta=\frac{1}{2}$ Na/GaAs(110) at the \bar{X}' point of the surface Brillouin zone [see Fig. 5(b)]. Lower panels give a side view and upper panels give a top view along a plane indicated in the lower panel by dashed lines. Large solid circle indicates As atoms, Ga atoms are marked by small solid circles, and Na atoms are indicated with the cross hatched circles. Units are 10^{-3} bohr $^{-3}$. Left: the highest occupied state. Right: the lowest unoccupied state.

band gap, we varied its occupation. We have performed self-consistent calculations for the (fixed) equilibrium geometry of the $\Theta = \frac{1}{2}$ Na/GaAs(110) system, occupying this state with 0.5, 1.0, and 1.5 electrons. In the latter case one electron was taken from a delocalized orbital in the valence band about 2 eV below the valence-band top and placed in the dangling-bond orbitals on both sides of the slab. As a consequence we find that the dangling-orbital state moves up in energy. In the first case half an electron was removed from the dangling-bond orbitals of both sides of the slab and placed in a delocalized state of the conduction band. Due to its reduced occupation the surface state is now shifted towards the valence band, i.e., to higher binding energies. We found that the emptying of valence-band states or the filling of conduction-band states is the best way to perform accurate calculations in the super-cell approach, as this approach requires neutral cells. Such a change in the valence or the conduction band will not happen in reality. However, we confirmed that, if a delocalized state is taken, the shift of the highest occupied state is only weakly affected. We also applied alternative ways to neutralize the super cell, namely adding a constant charge density to the whole super cell and to put impurity atoms in the center of the GaAs slab. These calculations gave very similar results. Comparing all these calculations the Hubbard correlation energy U is obtained to be $U = (1.2 \pm 0.3)$ eV. This result agrees well with the correlation energy for localized surface states estimated by Klepeis and Harrison⁴⁰ from simple electrostatic screening considerations. The margin of error of our calculation is rather large because of different relative shifts in energy of the dangling-bond orbital at different k points and because of the different methods applied. An additional difficulty with the determination of U was that not only does the gap state shift, but also the width of the valence band is modified.

The calculated value of U includes the effects of adsorbate-substrate hybridization as well as the surface screening. Comparing the estimated value of the correlation energy with the bandwidth, we find that $U > W$. We therefore conclude that the Bloch picture is not appropriate but that the partially filled gap state is, in fact, a Hubbard system. Thus, using the calculated parameter in a Hubbard Hamiltonian would give that this state will split into two states: One of these states will be fully occupied and the other one will be empty. We therefore conclude that the Na/GaAs(110) system behaves nonmetallic for coverages less than or equal to one monolayer.

Although at small coverages ($\Theta = \frac{1}{4}$ and $\frac{1}{2}$) the Ga dangling-bond states are only partially occupied [Figs. 5(a) and 5(b)], the size of U/W suggests that an electron added to the system would in fact go into the next higher band. Indeed, with STM applying positive sample bias, which corresponds to tunneling from the tip into unoccupied surface states, the picture was different from that applying negative sample bias.¹⁰ The STM image with positive bias shows no evidence of the GaAs or Cs corrugation along the adatom chains. The authors attribute the lack of corrugation to a smaller resolution of the microscope due to a cesiated tip. From our results discussed in Sec. IV one could offer an alternative explanation, namely

that for the tunnel current from the tip to the sample the relevant surface state is a low-correlation Cs-like state, which is very extended and will not give a significant corrugation. In contrast, the sample-to-tip tunneling was due to the high-correlation, very localized Ga dangling-orbital-like state, which points out of the surface.

The photothreshold is the energy difference between the vacuum level and the valence-band maximum. For the clean surface it is calculated combining bulk and surface calculations.^{9,42} In the bulk calculation the top of valence band is determined relative to the averaged electrostatic potential which we will call "bulk potential" and in the surface calculation the vacuum level is determined relative to the averaged electrostatic potential of the central layer, which, for a sufficiently thick slab, is indeed identical to a bulk layer. Therefore, by combining both calculations we are able to determine the vacuum level relative to the valence-band maximum. The photothreshold for the clean relaxed surface is calculated as 5.43 eV (Ref. 9) [for the unrelaxed surface geometry (truncated bulk) the value would be 0.25 eV lower; see Fig. 8]. The variation of the photothreshold as a function of alkali coverage is evaluated from the variation of the macroscopic (layer-averaged) electrostatic potential⁴¹ as a function of coverage: First, the electrostatic potential of the slab is averaged parallel to the (110) surface, and then this averaged potential is convoluted with a window function $f(z)$ with a width of the bulk layer distance L , i.e., $f(z) = 1$ for $-L/2 \leq z \leq L/2$ and zero elsewhere.

Figure 8 shows the macroscopic electrostatic potential of the Na/GaAs(110) system for all coverages studied in this work relative to that of the clean relaxed surface. The sodium adsorption reduces the photothreshold by

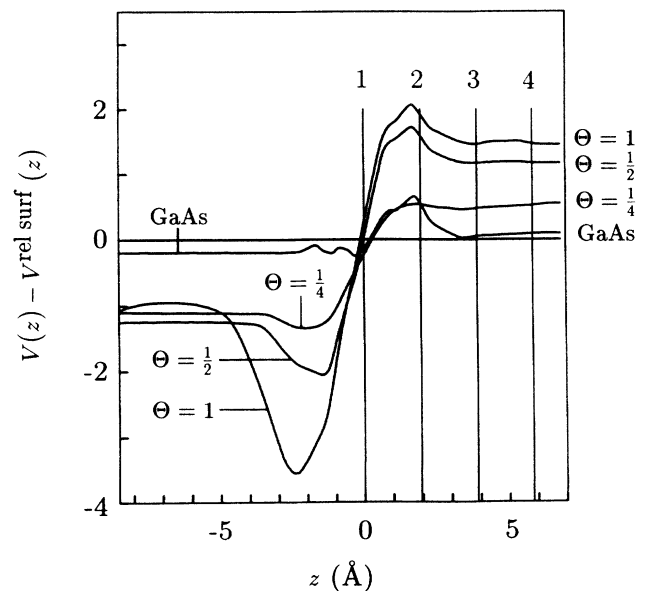


FIG. 8. Macroscopic electrostatic potential of the Na/GaAs(110) system for different coverages and of the clean unrelaxed surface, relative to the macroscopic electrostatic potential of the clean relaxed surface plotted as a function of distance z from the surface. The positions of the first four substrate layers are indicated by vertical bars.

about 2.4 eV for the $\Theta = \frac{1}{2}$ coverage. Increasing the coverage does not reduce the photothreshold further. Figure 9 shows the photothreshold as a function of coverage obtained from our results (diamonds) compared to experimental data obtained from photoemission measurements¹⁵ (solid line). Although the absolute value of the calculated photothreshold for the clean surface is smaller than the experimental value (for a discussion, see Ref. 9), the calculated variation of the photothreshold as a function of sodium coverage well reproduces the experimental results.

Analyzing the band structure of the Na/GaAs(110) system as a function of coverage, we can calculate the variation of the Schottky barrier. The p -type Schottky barrier is the energy difference between the Fermi level and the top of valence band. Our results are given in Table V. The Schottky barrier decreases with increasing sodium coverage. Thus we can reproduce the typical variation of the Schottky barrier in the range $\frac{1}{4} \leq \Theta \leq 1$.⁴³ The calculated values agree well with the experimental data for n -doped substrates.⁴³ The calculation enables us to analyze the origin of the change of the Schottky-barrier height with coverage. In the investigated range of coverage the shift of the Fermi level and thus the variation of the Schottky barrier is due to the coverage-dependent shift of the Ga derived surface state. Thus, there is no need to assume adsorbate-induced defects or surface chemical reactions to explain a Schottky-barrier behavior as that given in Table V.

Starting from our analysis, which shows that the electronic properties of Na/GaAs(110) in the submonolayer regime are determined by the Ga dangling-bond state, and taking into account that the energy of these dangling bonds changes with occupation, we can now speculate about the different behavior of the Schottky barriers for n - and p -type doped substrates in the very low coverage regime ($\Theta < 0.1$).

In the case of p -type materials the Fermi level is pinned by acceptor-impurity states close to the valence-band maximum. If we adsorb very few alkali atoms, the

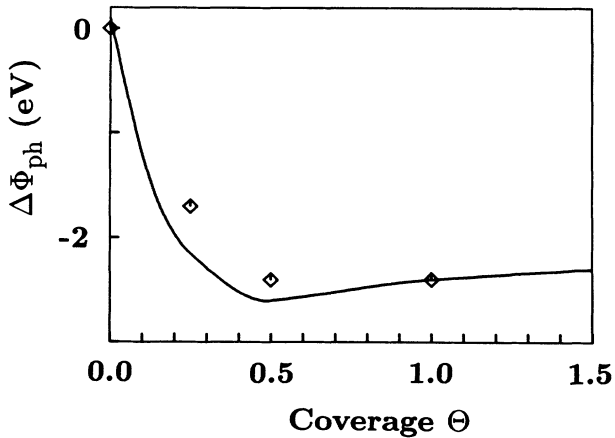


FIG. 9. Variation of the photothreshold $\Delta\Phi_{ph}$ as a function of alkali coverage. Diamonds represents the results obtained from the variation of the macroscopic electrostatic potential and the solid line represents the experimental data from Ref. 15.

TABLE V. Calculated photothreshold Φ_{ph} and (p -type) Schottky barrier Φ_B for different coverages of Na on GaAs(110).

| | Φ_{ph} (eV) | Φ_B (eV) |
|------------------------|---------------------|------------------|
| Clean surface | 5.43 | |
| $\Theta = \frac{1}{4}$ | 3.7 | 1.1 |
| $\Theta = \frac{1}{2}$ | 3.0 | 0.8 |
| $\Theta = 1$ | 3.0 | 0.6 |

adatom-induced states at the middle of the band gap will denote their electrons into the empty acceptor-impurity states. With increasing coverage we expect that the Fermi level shifts rapidly to the midgap (Ga dangling-bond) level, reaching this level when electrostatics prevents any additional electron transfer from the surface into acceptor-impurity states. The number of acceptor-impurity states which lie within the depth of band bending (i.e., typically 1000 Å) per unit surface area is very small, i.e., $\frac{1}{44}$ if the acceptor concentration is 10^{18} cm^{-3} . Thus, with the results of our calculation and without involving any adsorbate-induced defects or strong surface reaction, we predict that in p -type materials and $\Theta \approx 0.02$ the Fermi energy of the system should reach that of undoped material. Additional alkali adsorption pins the Fermi level at the Ga dangling bond and this level slowly changes with coverage up to the point where the adsorption process is changed into a three-dimensional growth of the alkali metal. Then the Fermi level stays fixed.

In the case of n -doped material, the Fermi level is near the bottom of the conduction band. The sodium adsorption induces partially occupied states in the middle of the band gap but our calculations predict that the electrons from the Fermi level will not go into these states because of the large correlation repulsion. Even if the calculation would overestimate the correlation energy U , which then may enable the donor-impurity electrons to occupy the surface state, it will certainly move up in energy upon occupation, giving a Fermi level again close to the conduction-band minimum.

When for p -type material all acceptor impurities which lie in the range of band bending are saturated, then the variation of the Fermi level and the local electronic structure at the surface are similar to that in the case of n -type materials.

VI. SUMMARY

We applied DFT-LDA to calculate the electronic structure and the atomic geometry for sodium-covered GaAs(110) by total-energy minimizations using a Car-Parrinello-like technique.³⁰ It turns out that the atomic geometry at the surface strongly depends on the alkali coverage. For submonolayer coverages the clean surface relaxation is partially undone only at the adsorbate nearest neighbors. A full monolayer sodium coverage essentially removes the relaxation of the substrate and increases the layer spacing between first and second substrate layer by about 6%. The topology of the total-energy surface indicates that sodium atoms can move rather freely on the GaAs(110) surface but the diffusion

will be highly anisotropic, i.e., a sodium atom migrates along the $[1\bar{1}0]$ direction. We have found different adsorption positions for different coverages. At low coverages, i.e., $\Theta \leq \frac{1}{4}$, the sodium adsorption close to a surface Ga atom is most favorable. The adsorbate-induced state is mainly built from the Ga dangling orbital with little Na $3s$ character. The sodium $3s$ electron is transferred into this orbital, which results in an adsorbate-induced dipole moment, which lowers the photothreshold. For higher sodium coverages, $\Theta = \frac{1}{2}$ in the (1×1) structure, the adsorption at a surface Ga or As atom yields the same adsorption energy. In the case of the full monolayer coverage we find that one adatom is adsorbed bridging two Ga atoms in the $[00\bar{1}]$ direction and the other one bridges two consecutive Ga atoms in the $[1\bar{1}0]$ direction, which results in a significantly buckled Na layer. We note, however, that for this coverage also other adatom arrangements may be possible. The adsorption energy per adsorbate atom is very similar for all coverages studied in this paper, however for the coverage $\Theta = \frac{1}{2}$ the calculations give a slightly less favorable energy, $\Delta E \approx 0.1$ eV. This difference is close to the numerical accuracy of our calculations. Nevertheless we tend to conclude that at low coverages the adsorption happens in an open structure but for higher adsorbate concentration a local coverage of one monolayer is preferred.

For three coverages and using the atomic geometry, which gives the lowest total energy, we have analyzed the electronic structure in detail. In particular, we discuss how for the different atomic geometries the electronic structure changes. For submonolayer coverages we have found that the highest occupied states are partially filled Ga dangling-bond-like states which are strongly local-

ized. These states are responsible for the Fermi-level pinning. For intrinsic and n -type material, the Na adsorbate donates its electron into this surface state. For p -type materials at the very initial stage of adsorption, the Na valence electron is, however, donated into the acceptor impurity states. These results explain the difference in n -type and p -type behavior of Schottky barrier without the need to invoke adsorbate-induced defects or an unusual "adsorbate-substrate chemical reaction." The calculated Schottky-barrier heights at different coverages as well as the variation of the photothreshold agree well with recent experimental results. The character of the state responsible for the Fermi-level pinning is similar to that of the empty Ga dangling-bond orbital of the clean GaAs(110) surface. We find that because of its localized character these states should be described in a Hubbard picture rather than in a Bloch picture: The calculated Hubbard correlation energy U is clearly bigger than the calculated bandwidth. We therefore expect that the state will split into two states if we consider the correlation repulsion in the many-particle Hamiltonian. As a consequence, the systems should behave nonmetallically. At one monolayer and higher coverage the system electronic properties are determined by Na states.

ACKNOWLEDGMENTS

We thank Martina Heinemann for collaboration in the initial stage of this work and Roland Stumpf for help with the computer code. We gratefully acknowledge stimulating discussions with Friedhelm Bechstedt and Oleg Pankratov. This work was supported in part by the Stiftung Volkswagenwerk.

*Permanent address: AGFA Laborgeräte GmbH Gera, Keplerstrasse 100, O-6500 Gera, Germany.

¹L. J. Brillson, *Surf. Sci. Rep.* **2**, 123 (1982).

²E. H. Roderick and R. H. Williams, *Metal-Semiconductor Contacts* (Clarendon, Oxford, 1988).

³V. Heine, *Phys. Rev.* **138**, A1689 (1965).

⁴C. Tejedor, F. Flores, and E. Louis, *J. Phys. C* **10**, 2163 (1977).

⁵W. A. Harrison and J. Tersoff, *J. Vac. Sci. Technol. B* **4**, 1068 (1986).

⁶W. E. Spicer, I. Lindau, P. Skeath, and C. Y. Su, *J. Vac. Sci. Technol.* **17**, 1019 (1980).

⁷W. E. Spicer, T. Kendelewicz, N. Newman, R. Cao, C. McCants, K. Miyano, I. Lindau, and E. R. Weber, *Appl. Surf. Sci.* **33/34**, 1009 (1988).

⁸W. Mönch, *Rep. Prog. Phys.* **53**, 221 (1990).

⁹J. L. Alves, J. Hebenstreit, and M. Scheffler, *Phys. Rev. B* **44**, 6188 (1991).

¹⁰P. N. First, R. A. Dragoset, J. A. Stroschio, R. J. Celotta, and R. M. Feenstra, *J. Vac. Sci. Technol. A* **7**, 2868 (1989).

¹¹L. J. Whitman, J. A. Stroschio, R. A. Dragoset, and R. J. Celotta, *Phys. Rev. Lett.* **66**, 1338 (1991).

¹²J. E. Ortega and R. Miranda (unpublished).

¹³N. J. DiNardo, T. Meada Wong, and E. W. Plummer, *Phys. Rev. Lett.* **65**, 2177 (1990); note the different definition of one monolayer.

¹⁴T. Maeda Wong, N. J. DiNardo, D. Heskett, and E. W. Plum-

mer, *Phys. Rev. B* **65**, 12342 (1990); note the different definition of one monolayer.

¹⁵M. Prietsch, M. Domke, C. Laubschat, T. Mandel, C. Xue, and G. Kaindl, *Z. Phys. B* **74**, 21 (1989).

¹⁶R. Cao, K. Miyano, T. Kendelewicz, I. Lindau, and W. E. Spicer, *Phys. Rev. B* **39**, 12655 (1989).

¹⁷K. O. Magnusson and B. Reihl, *Phys. Rev. B* **40**, 7814 (1989); **40**, 5864 (1989).

¹⁸J. Ortega and F. Flores, *Phys. Rev. Lett.* **63**, 2500 (1989).

¹⁹C. Y. Fong, L. H. Yang, and I. P. Batra, *Phys. Rev. B* **40**, 6120 (1989).

²⁰P. Hohenberg and W. Kohn, *Phys. Rev.* **136**, B864 (1964).

²¹W. Kohn and L. J. Sham, *Phys. Rev.* **140**, A1133 (1965).

²²D. M. Ceperley and B. A. Alder, *Phys. Rev. Lett.* **45**, 566 (1980).

²³J. P. Perdew and A. Zunger, *Phys. Rev. B* **23**, 5048 (1981).

²⁴S. G. Louie, S. Froyen, and M. L. Cohen, *Phys. Rev. B* **26**, 1738 (1982).

²⁵X. Gonze, P. Käckell, and M. Scheffler, *Phys. Rev. B* **41**, 12264 (1990).

²⁶X. Gonze, R. Stumpf, and M. Scheffler, *Phys. Rev. B* **44**, 8503 (1991).

²⁷M. Schlüter, J. R. Chelikowsky, S. G. Louie, and M. L. Cohen, *Phys. Rev. B* **12**, 4200 (1975).

²⁸H. J. Monkhorst and J. D. Pack, *Phys. Rev. B* **13**, 5188 (1976).

²⁹J. Hebenstreit, M. Heinemann, and M. Scheffler, *Phys. Rev.*

- Lett. **67**, 1031 (1991).
- ³⁰R. Car and M. Parrinello, Phys. Rev. Lett. **55**, 2471 (1985).
- ³¹G. B. Bachelet, D. R. Hamann, and M. Schlüter, Phys. Rev. B **26**, 4199 (1982).
- ³²*Handbook of Chemistry and Physics*, 67th ed., edited by R. C. Weast (CRC, Boca Raton, 1986).
- ³³S. Froyen and M. L. Cohen, Phys. Rev. B **29**, 3770 (1984).
- ³⁴C. Y. Fong and M. L. Cohen, Phys. Rev. Lett. **21**, 22 (1968).
- ³⁵S. Froyen and M. L. Cohen, J. Phys. C **19**, 2623 (1986).
- ³⁶V. L. Moruzzi, J. F. Janak, and A. R. Williams, *Calculated Electronic Properties of Metal* (Pergamon, New York, 1976).
- ³⁷J. T. Lewis, A. Lehoczki, and C. V. Briscoe, Phys. Rev. **161**, 877 (1967).
- ³⁸In Ref. 32 the Na-Na bond length at 20°C is given. Along with the coefficient of linear thermal expansion ($\alpha = 7 \times 10^{-5} \text{ K}^{-1}$) the lattice constant at zero temperature is extrapolated.
- ³⁹C. Kittel, *Introduction to Solid Physics*, 6th ed. (Wiley, New York, 1986).
- ⁴⁰J. E. Klepeis and W. A. Harrison, J. Vac. Sci. Technol. B **7**, 964 (1989).
- ⁴¹A. Baldereschi, S. Baroni, and R. Resta, Phys. Rev. Lett. **61**, 734 (1988).
- ⁴²Guo-Xin Qian, R. M. Martin, and D. J. Chadi, Phys. Rev. B **37**, 1303 (1988).
- ⁴³M. Prietsch, C. Laubschat, M. Domke, and G. Kaindl, Europhys. Lett. **6**, 451 (1988).

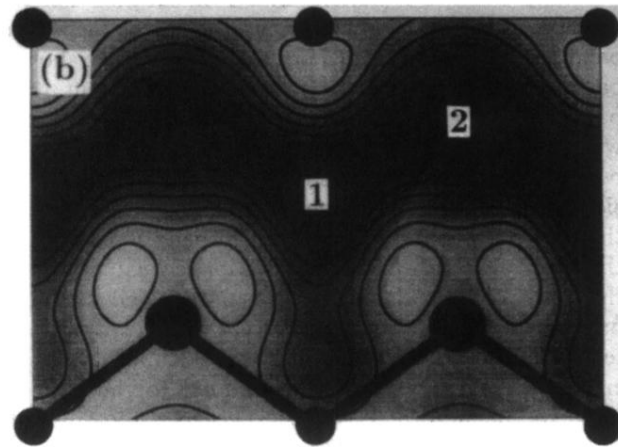
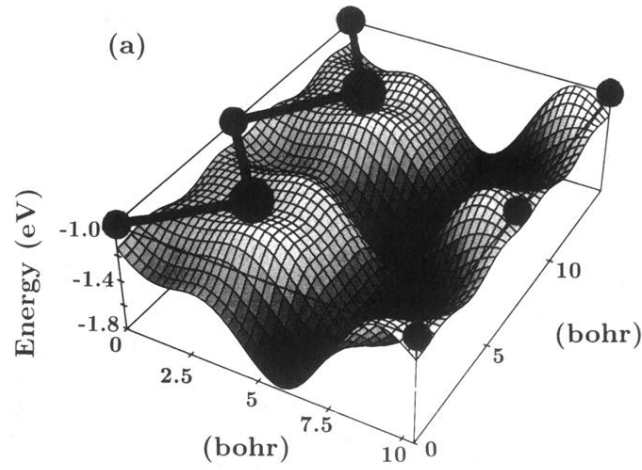


FIG. 4. Total-energy surface of the $\Theta = \frac{1}{2}$ Na/GaAs(110) system. (a) Three-dimensional perspective view and (b) contour plot together with the projected surface atomic positions. Large circles indicate As atoms and small circles mark the Ga atoms. In the contour plot the channel in the total-energy surface is drawn dark grey. The labels "1" and "2" indicate stable adsorption positions for the $\Theta = \frac{1}{2}$ coverage.